International Journal of Theoretical Physics (2025) 64:64
https://doi.org/10.1007/s10773-025-05937-3

RESEARCH

Exploring the Gross-Pitaevskii Model in Bose-Einstein Condensates and Communication Systems: Features of Solitary Waves and Dynamical Analysis

Muhammad Ajmal[1] · Jan Muhammad[1] · Usman Younas[1] · Ejaz Hussian[2] · Mohammed El- Meligy[3,4] · Mohamed Sharaf[5]

Received: 14 November 2024 / Accepted: 22 February 2025

Abstract

The Gross-Pitaevskii Equation (GPE), which belongs to the class of nonlinear Schrödinger equations is recognized for its applications in diverse fields such as Bose-Einstein Condensates and optical fiber. In this study, the dynamic behaviors of various wave solutions to the M-fractional nonlinear Gross-Pitaevskii equation are examined. Intriguing insights into the mechanisms regulating the intricate wave patterns of the model are offered through this investigation. To secure the solutions, including complex, bright, dark, combined, and singular soliton solutions, the Kumar-Malik method, the modified generalized exponential rational function method, and the generalized multivariate exponential rational integral function method are substantially applied. The fractional parametric effects on solitary waves are observed graphically. Moreover, the Galilean transformation is adopted, and bifurcation, sensitivity, chaotic behavior, 2D and 3D phase portraits, Poincaré maps, time series analysis, and sensitivity to multistability under different conditions are explored.

Keywords M-fractional derivatives · Solitons · Nonlinear Gross-Pitaevskii equation · Mathematical methods · Qualitative analysis · Multistability

1 Introduction

In today's scientific and technological era, the study of nonlinear wave phenomena is gaining increasing interest among scientists and engineers. Nonlinear partial differential equations (NLPDEs) effectively characterize a diverse array of fields in engineering and research, including plasma physics, optical fiber technology, acoustics, finance, turbulence, mechani-

✉ Usman Younas
usmanalgebra@shu.edu.cn; usmanalgebra1@yahoo.com

1 Department of Mathematics, Shanghai University, No. 99 Shangda Road, 200444 Shanghai, China

2 Department of Mathematics, University of the Punjab, Lahore, Pakistan

3 Applied Science Research Center, Applied Science Private University, Amman, Jordan

4 Jadara University Research Center, Jadara University, PO Box 733, Irbid, Jordan

5 Department of Industrial Engineering, College of Engineering, King Saud University, Riyadh 12372, Saudi Arabia

Published online: 28 February 2025

cal engineering, control theory, and nonlinear biological systems [1, 2]. The investigation of exact solutions to nonlinear equations is a critical component of the investigation of nonlinear physical processes. NLPDEs are frequently used to model nonlinear physical phenomena. In comparison, researchers encounter an enormous challenge when confronted with nonlinearity. Numerous authors from various disciplines have addressed this challenge by developing a variety of numerical and analytical methods to identify potential solutions to nonlinear equations. These high-order classes of NLPDEs prevent the standardization of NLPDE solutions. Therefore, there are specific methodologies that can solve complex PDEs within specific constraints. PDEs that illustrate the dynamics of a system's evolution over time are known as evolution PDEs. The process by which a system transforms or evolves is represented by evolutionary PDEs, which incorporate time as a factor. Dynamic process modeling is frequently employed to implement evolution PDEs in a variety of disciplines, such as engineering, biology, economics, and physics. An understanding of these equations is necessary to comprehend the behavior of physical systems, as they demonstrate the progression of variables such as temperature, displacement, or wave function over time and space. The advancement of straightforward analytical solutions to the complex relationship that exists between the rate of change of a variable in these nonlinear equations is frequently influenced by complexity. In contrast to their linear counterparts, these equations provide a more accurate representation of the underlying dynamics by illustrating the complex interactions between a variety of variables. Fractional differential equations are encountered in a variety of fields, such as engineering, social sciences, and fundamental sciences [3]. Their substantial contributions to a variety of disciplines that necessitate complex physical processes, such as control theory, electrical circuits, and wave propagation, have recently garnered an increasing amount of attention [4]. A wide range of technical challenges are modeled and designed using these equations [5]. The solutions to these equations have been advantageous in that they offer a comprehensive understanding of nonlinear physical properties and suggest a new direction for future research.

More importantly, solitons are regarded as one of the most intriguing research areas and have an extensive variety of applications in nonlinear sciences. As a consequence of its relevance to contemporary research in telecommunications engineering and mathematical physics, the scientific community has nurtured an interest in the theory of optical solitons. Soliton waves are capable of traveling vast distances without losing their shape as a result of dispersion. Thus, they are indispensable in the subject of nonlinear technology. Research is performed to further investigate the development and testing of solitons. Construction of soliton solutions is the sole approach to investigating these equations, as they exhibit unique behaviors. A rapidly evolving subfield within the field of telecommunications is the theory of solitons. A wide range of electronic manufacturing applications, including magneto-optics, birefringent fibers, metamaterials, and others, have the potential to use soliton technology. Photopolymers, bulk materials, optical waveguides, and photonic crystal fibers are among the systems in which solitons may be present [6]. There are numerous studies that have demonstrated the wide variety of attributes of soliton solutions and their practical applications in scientific and technological fields [7]. Soliton solutions are implemented in a variety of fields, including nonlinear optics, coastal engineering, plasma physics, communication engineering, and fluid dynamics [8]. An extensive variety of numerical and analytical algorithms have been devised by mathematicians to identify soliton solutions for the NLPDEs. In order to investigate novel applications and advance these disciplines, researchers may develop a more comprehensive understanding of solitons.

In a multiplicity of physical systems, exact solutions are regarded as of paramount importance, as they enable the analysis of physical behaviors and establish a foundation for subsequent research and investigation. A common way of obtaining an exact solution is to characterize the behaviors of a physical system as an ODE or PDE. NLPDEs or FNLPDEs can be employed to simulate a variety of intricate natural or industrial phenomena. Many researchers have devised numerous methodologies and strategies to resolve these issues with precision. The following strategies are among the most frequently employed and widely recognized that have been recently developed: Hirota bilinear method [9], multiple exp-function approach [10], Lie classical approach [11], truncated Painlevé approach [12], Riccati equation mapping method [13], Adomian decomposition technique [14], Lie symmetry technique [15], Darboux transformation [16], Bernoulli $\frac{G'}{G}$-expansion method [17], bifurcation analysis [18, 19], $\frac{G'}{G}$-expansion method [20], modified Sardar subequation method [21], modified simple equation technique [22], iterative transform method [23], $tan(\frac{\phi}{2})$ technique [24], simplest equation technique [25] etc.

Furthermore, a dynamical system is an equation that depicts the evolution of a system through time. This system's constituent differential equations describe the time-dependent behavior of the system. Many fields use dynamic systems to study the behavior of complex systems. These fields include engineering, biology, economics, ecology, physics, and engineering. Basic dynamical systems include the stock market, the planets in a solar system, the motion of a pendulum, and the dynamics of a species' population. The dynamical system relies on the idea of bifurcation analysis theory. Dynamical systems exhibit qualitative modifications in the behavior of distributed systems as a result of modifications to system parameters. When a system's behavior undergoes a sudden change, a bifurcation may happen [26]. When two unstable equilibrium points collide with one stable equilibrium point, it is possible for the stability of the equilibrium points to switch places. Two stable equilibrium points break apart and one unstable equilibrium point is created in the case of this collision. In many fields, including engineering, biology, economics, and physics, bifurcation theory is used to understand the behavior of nonlinear dynamical systems. In addition, the chaos theory delves into the study of deterministic systems that, although being controlled b basic mathematical equations, display intricate and surprising behavior [27]. Even small changes to the starting conditions can have a big impact on the final outcome. The phase space of the system is finally defined by the path taken by neighboring points. An infinite number of periodic orbits are densely packed into the system's phase space. Some well-known examples of chaotic systems include the fluid movement, the logistic map, weather, and double pendulum. Numerous disciplines have made use of chaos theory, including the social sciences, economics, engineering, biology, and physics. It has changed the way we think about deterministic systems and how we perceive natural randomness and predictability [28]. Instead of illustrating the entire trajectory, the Poincaré maps, also known as Poincaré sections emphasize the points at which the trajectory intersects the plane, thereby offering a more comprehensive understanding of potential bifurcations, stability features, and periodic orbits. This methodology provides a comprehensive visualization of the system's dynamics, enabling the identification of stability characteristics, periodicity, and transitions to more intricate behaviors.

This work mainly aims to investigate the complex dynamics behaviors inherent in the fractional nonlinear Gross-Pitaevskii equation applying the analytical approaches like Kumar-Malik method [29], the modified generalized exponential rational function method (mGERFM) [30], and the multivariate generalized exponential rational integral function method (MGERIFM) [31] and analyzing its nonlinear dynamical behavior in the forms of bifurcation analysis, chaotic behavior, Poincaré maps, time series analysis, and sensitivity to multistability. The purpose of these objectives is to enhance our understanding of the behavior of the proposed model and to address the challenges posed by highly complex mathematical models. The applied approaches are highly effective due to the structured framework that is provided for the system of nonlinear complex models, as well as its simplicity, and capacity to produce a diverse array of novel results.

The remaining article is organized as follows: In Section 2, a variety of the most significant properties and fundamental concepts that are associated with fractional derivatives are discussed. The governing model is introduced in Section 3, and soliton solutions are computed in Section 4 using integration approaches such as the Kumar-Malik method, the mGERFM, and the MGERIFM. The solutions are visually represented in Section 5, while the concluding remarks are the main focus of Section 6.

2 Fractional Order Derivatives

Fractional calculus (FC) is generally considered to be a field in which the integral and derivative of fractional order are prevalent topics due to their numerous potential applications in various fields of science. This subject has attracted substantial interest from researchers due to its prevalence and importance in the modeling of a diverse array of natural processes. FC and its applications in a variety of disciplines have been the subject of extensive research by scholars. Fractional differential equations are a practical and efficient approach to the description of natural phenomena. It captivates both pure and applied mathematicians. Mathematicians who specialize in pure mathematics are investigating the existence and uniqueness of solutions to fractional differential equations. Applied mathematics research on fractional partial differential equations (FPDEs) contain numerical solutions and propagating waves, are essential for understanding many natural nonlinear physical processes and are important in the nonlinear sciences. Data processing, viscoelasticity, electrode electrolyte polarization, electromagnetic waves, glass fiber, plasma physics, biogenetics, solid physics, circuits, and control theory are among the numerous applications of FPDEs. The examination of traveling wave solutions significantly enhances our comprehension of the behaviors of a wide range of nonlinear problems in physical science. A diverse array of methodologies that are both effective and robust have been proposed in the literature to evaluate the soliton and solitary wave solutions of FPDEs. Recent fractional calculus research has shown that fractional models often better capture physical events than integer models.The M-truncated fractional derivative represents a modified form of the fractional derivative that introduces a truncation parameter, offering a practical approach to handle the non-locality of traditional fractional derivatives. Physically, it accounts for the influence of fractional-order dynamics within a finite range, which is particularly useful in modeling systems where long-range interactions are limited or where localized behavior is of interest. This study employs the proposed model as an illustration to assess the efficacy of fractional derivatives as a tool for investigating and understanding specific physical phenomena.

The truncated M-fractional derivative

Definition 2.1 For $f : [0, \infty) \to \mathbb{R}$, the truncated M-fractional derivative [32] is described by:

$$\mathscr{D}_M^{\omega,\,\mu}\{(f)(t)\} = \lim_{\epsilon \to 0} \frac{f(t\mathbb{E}_\mu(\epsilon t^{1-\omega})) - f(t)}{\epsilon}, \quad \mu > 0,\ \omega \in (0, 1),\ \forall t > 0, \tag{1}$$

where $\mathbb{E}_\mu(.)$ is the parameter of truncated Mittag-Leffler function [32].

Theorem 2.1 *If $\mu > 0$, $0 < \omega < 1$, $p, \ s \in \mathbb{R}$, and f, ρ are differentiable at the given point $t > 0$. Then:*

1. $\mathscr{D}_M^{\omega,\ \mu}\{(p\rho + sf)(t)\} = p\mathscr{D}_M^{\omega,\ \mu}\{\rho(t)\} + s\mathscr{D}_M^{\omega,\ \mu}\{f(t)\}$.
2. $\mathscr{D}_M^{\omega,\ \mu}\{(\rho\ .\ f)(t)\} = \rho(t)\mathscr{D}_M^{\omega,\ \mu}\{f(t)\} + f(t)\mathscr{D}_M^{\omega,\ \mu}\{\rho(t)\}$.
3. $\mathscr{D}_M^{\omega,\ \mu}\{\frac{\rho}{f}(t)\} = \frac{f(t)\mathscr{D}_M^{\omega,\ \mu}\{\rho(t)\} - \rho(t)\mathscr{D}_M^{\omega,\ \mu}\{f(t)\}}{[f(t)]^2}$.
4. $\mathscr{D}_M^{\omega,\ \mu}\{c\} = 0$, *with $\rho(t) = c$ being the constant.*
5. *If ρ is differentiable, then $\mathscr{D}_M^{\omega,\ \mu}\{\rho(t)\} = \frac{t^{1-\omega}}{\Gamma(\mu+1)}\frac{d\rho(t)}{dt}$.*

3 The Governing Equation

The rapid theoretical and experimental advancements in ultracold physics have garnered significant attention in the past two decades, particularly in the study of quantum liquids, including Bose-Einstein condensates (BEC), helium, and ultracold Fermi gases [33]. The nonlinearity that comes from particle interactions is one of the most interesting things about BEC that has sparked a lot of interest in both theoretical research and experimental testing. The confinement potentials, which are typically harmonic, significantly influence this nonlinearity. The magnetically controlled Feshbach resonance approach has made it possible to continuously adjust the sign and intensity of inter-particle interactions, which can range from positive to negative infinity. The capability of degenerate Fermi gases at ultracold temperatures has made the long-awaited Bardeen-Cooper-Schrieffer-BEC crossover possible. As a result, BEC has developed into a versatile platform for investigating nearly any aspect of modern physics, including condensed matter physics and astrophysics. The GPE, which is an important part of mean field theories, has shown a remarkable level of accuracy in describing how BEC moves. Extensive studies from both mathematical and physical perspectives have yielded significant insights, and numerous researchers have identified exact solutions that exhibit various forms of solitons. The recent increase in interest in cold atomic Fermi gases has coincided with the introduction of the generalized GPE to derive analytical solutions for dynamic behaviors. The important model, namely GGPE, is described by [34]

$$i\frac{\partial}{\partial t}\varphi(x,t) = -\frac{\partial^2}{\partial x^2}\varphi(x,t) - \frac{1}{2}\varepsilon^2x^2\varphi(x,t) + 2M\frac{p_s}{L_\perp}|\varphi(x,t)|^2\varphi(x,t), \tag{2}$$

where $\varepsilon << 1$, M is a real constant and p_s is used to denote the frequency of the harmonic oscillator. The wave function of BEC is denoted by $U(x,t)$

$$\varphi(x,t) = U(x,t)e^{\frac{i\varepsilon t}{2} - \frac{\varepsilon x^2}{4}}, \tag{3}$$

where $t = 2\int_0^t e^{2\varepsilon\tau}d\tau$ and $x = xe^{\varepsilon t}$. The M-fractional form of nonlinear GPE read as

$$i\mathscr{D}_{M,t}^{\omega,\ \mu}U + \frac{1}{2}\mathscr{D}_{M,x}^{2\omega,\ \mu}U - d|U^2|U = 0, \tag{4}$$

where $d = M\frac{p_0}{L_\perp}$ and $U = U(x,t)$. Equation 4 is derived from the magnetic field theory, which is observed by magnetically modulating the inter-atomic interaction. Moreover, the literature examines this model from different perspectives, such as in [34] the exact solutions are studied applying the rational sine-Gordon expansion method where in [35] the Hirota bilinear approach is applied to extract various soliton solutions. While in [36] the proposed model was studied with conformable derivatives of beta type applying sub-equation method.

4 Extraction of Solutions

Solution of (4) may be obtained using the transformation defined by:

$$U = \Phi(\xi) e^{\frac{i\Gamma(\beta+1)(cx^{\omega}-bt^{\omega})}{\omega}}; \tag{5}$$

$$\xi = \frac{\Gamma(\beta+1)\left(ax^{\omega}-\kappa t^{\omega}\right)}{\omega}, \tag{6}$$

where the parameters $a,\ b,\ c,\ \kappa$ are real constants. By integrating the predefined transformations in (4), we have

$$\textbf{Real Part:} \qquad a^2\Phi^{''}(\xi) + \left(2b - c^2\right)\Phi(\xi) - 2d\Phi^3(\xi) = 0, \tag{7}$$

$$\textbf{Imaginary Part:} \qquad \kappa\Phi^{'}(\xi) - ac\Phi^{'}(\xi) = 0. \tag{8}$$

We get $\kappa = ac$ from the (8).

Homogeneous Balance principle:

The homogeneous balance principle states that the comparison between the highest order of linear derivative term and the highest degree of nonlinear term as follows:

$$\frac{d^p\Phi}{d\xi^p} = n + p \tag{9}$$

$$\Phi^p\left(\frac{d^q\Phi}{d\xi^q}\right)^s = np + s(n+q) \tag{10}$$

Following that, the homogeneous balancing principle between the terms Φ^3 and Φ'' in (7) results as follows:

$$\Phi'' = n + 2 \tag{11}$$

$$\Phi^3 = 3n \tag{12}$$

By comparing the (11) and (12), $\implies\ n+2 = 3n,\ \implies\ n = 1$ we obtain the value of $n = 1$, which is positive integer.

4.1 Kumar-Malik Method

For $n = 1$ the general solution of Kumar-Malik method [29] can be described as

$$\Phi(\xi) = \alpha_0 + \alpha_1\Omega(\xi), \tag{13}$$

with

$$\Omega^{'}(\xi) = \sqrt{\lambda_1\Omega(\epsilon)^4 + \lambda_2\Omega(\epsilon)^3 + \lambda_3\Omega(\epsilon)^2 + \lambda_4\Omega(\epsilon) + \lambda_5}. \tag{14}$$

The following solutions are obtained by employing (13) along with (14) in (7):

- **Case-1** For $\lambda_5 \rightarrow \frac{(4\lambda_1\lambda_3-\lambda_2^2)^2}{64\lambda_1^3}$, $\lambda_4 \rightarrow \frac{\lambda_2(4\lambda_1\lambda_3-\lambda_2^2)}{8\lambda_1^2}$ offers $\alpha_1 = \frac{4\alpha_0\lambda_1}{\lambda_2}$, $b = \frac{3a^2\lambda_2^2-8a^2\lambda_1\lambda_3+8c^2\lambda_1}{16\lambda_1}$, $d = \frac{a^2\lambda_2^2}{16\alpha_0^2\lambda_1}$. As a result we have the following solutions:

When $\lambda_1 > 0$ and $8\lambda_1\lambda_3 - 3\lambda_2^2 < 0$, we get: The dark soliton solution as follows:

$$U_1(x,t) = e^{\left(\frac{i\Gamma(\beta+1)\left(cx^{\omega}-\frac{t^{\omega}\left(3a^2\lambda_2^2-8a^2\lambda_1\lambda_3+8c^2\lambda_1\right)}{16\lambda_1}\right)}{\omega}\right)}\left(-\frac{\alpha_0\sqrt{3\lambda_2^2-8\lambda_1\lambda_3}\tanh\left(\frac{\sqrt{\lambda_1(3\lambda_2^2-8\lambda_1\lambda_3)}\xi}{4\lambda_1}\right)}{\lambda_2}\right), \tag{15}$$

The singular soliton solution

$$U_2(x,t) = e^{\left(\frac{i\Gamma(\beta+1)\left(cx^{\omega}-\frac{t^{\omega}\left(3a^2\lambda_2^2-8a^2\lambda_1\lambda_3+8c^2\lambda_1\right)}{16\lambda_1}\right)}{\omega}\right)}\left(\frac{\alpha_0\sqrt{3\lambda_2^2-8\lambda_1\lambda_3}\coth\left(\frac{\sqrt{\lambda_1(3\lambda_2^2-8\lambda_1\lambda_3)}\xi}{4\lambda_1}\right)}{\lambda_2}\right). \tag{16}$$

When $\lambda_1 > 0$ and $8\lambda_1\lambda_3 - 3\lambda_2^2 > 0$, we get the explicit silitary periodic solutions as follows:

$$U_3(x,t) = e^{\left(\frac{i\Gamma(\beta+1)\left(cx^{\omega}-\frac{t^{\omega}\left(8\lambda_1(c^2-a^2\lambda_3)+3a^2\lambda_2^2\right)}{16\lambda_1}\right)}{\omega}\right)}\left(\frac{\alpha_0\sqrt{8\lambda_1\lambda_3-3\lambda_2^2}\tan\left(\frac{\sqrt{\lambda_1(8\lambda_1\lambda_3-3\lambda_2^2)}\xi}{4\lambda_1}\right)}{\lambda_2}\right), \tag{17}$$

$$U_4(x,t) = e^{\left(\frac{i\Gamma(\beta+1)\left(cx^{\omega}-\frac{t^{\omega}\left(8\lambda_1(c^2-a^2\lambda_3)+3a^2\lambda_2^2\right)}{16\lambda_1}\right)}{\omega}\right)}\left(\frac{\alpha_0\sqrt{8\lambda_1\lambda_3-3\lambda_2^2}\cot\left(\frac{\sqrt{\lambda_1(8\lambda_1\lambda_3-3\lambda_2^2)}\xi}{4\lambda_1}\right)}{\lambda_2}\right). \tag{18}$$

- **Case-2** For $\lambda_5 \rightarrow \frac{\lambda_2^2(16\lambda_1\lambda_3-5\lambda_2^2)}{256\lambda_1^3}$, $\lambda_4 \rightarrow \frac{\lambda_2(4\lambda_1\lambda_3-\lambda_2^2)}{8\lambda_1^2}$ offers $\alpha_1 = \frac{4\alpha_0\lambda_1}{\lambda_2}$, $b = \frac{3a^2\lambda_2^2-8a^2\lambda_1\lambda_3+8c^2\lambda_1}{16\lambda_1}$, $d = \frac{a^2\lambda_2^2}{16\alpha_0^2\lambda_1}$. As a result we have the following solutions:

When $\lambda_1 < 0$ and $8\lambda_1\lambda_3 - 3\lambda_2^2 < 0$, we get the bright soliton solution as follows:

$$U_5(x,t) = e^{\left(\frac{i\Gamma(\beta+1)\left(cx^{\omega}-\frac{t^{\omega}\left(8\lambda_1(c^2-a^2\lambda_3)+3a^2\lambda_2^2\right)}{16\lambda_1}\right)}{\omega}\right)}\left(\frac{\alpha_0\sqrt{6\lambda_2^2-16\lambda_1\lambda_3}\,\mathrm{sech}\left(\frac{\sqrt{\lambda_1(8\lambda_1\lambda_3-3\lambda_2^2)}\xi}{2\sqrt{2}\lambda_1}\right)}{\lambda_2}\right). \tag{19}$$

When $\lambda_1 > 0$ and $8\lambda_1\lambda_3 - 3\lambda_2^2 > 0$, we get the singular soliton solution as:

$$U_6(x,t) = e^{\left(\frac{i\Gamma(\beta+1)\left(cx^{\omega}-\frac{t^{\omega}\left(8\lambda_1\left(c^2-a^2\lambda_3\right)+3a^2\lambda_2^2\right)}{16\lambda_1}\right)}{\omega}\right)}\left(\frac{\alpha_0\sqrt{16\lambda_1\lambda_3-6\lambda_2^2}\operatorname{csch}\left(\frac{\sqrt{\lambda_1\left(8\lambda_1\lambda_3-3\lambda_2^2\right)}\xi}{2\sqrt{2}\lambda_1}\right)}{\lambda_2}\right). \tag{20}$$

When $\lambda_1 > 0$ and $8\lambda_1\lambda_3 - 3\lambda_2^2 < 0$, we get the periodic solutions as:

$$U_7(x,t) = e^{\left(\frac{i\Gamma(\beta+1)\left(cx^{\omega}-\frac{t^{\omega}\left(8\lambda_1\left(c^2-a^2\lambda_3\right)+3a^2\lambda_2^2\right)}{16\lambda_1}\right)}{\omega}\right)}\left(\frac{\alpha_0\sqrt{6\lambda_2^2-16\lambda_1\lambda_3}\sec\left(\frac{\sqrt{\lambda_1\left(3\lambda_2^2-8\lambda_1\lambda_3\right)}\xi}{2\sqrt{2}\lambda_1}\right)}{\lambda_2}\right), \tag{21}$$

$$U_8(x,t) = e^{\left(\frac{i\Gamma(\beta+1)\left(cx^{\omega}-\frac{t^{\omega}\left(8\lambda_1\left(c^2-a^2\lambda_3\right)+3a^2\lambda_2^2\right)}{16\lambda_1}\right)}{\omega}\right)}\left(\frac{\alpha_0\sqrt{6\lambda_2^2-16\lambda_1\lambda_3}\csc\left(\frac{\sqrt{\lambda_1\left(3\lambda_2^2-8\lambda_1\lambda_3\right)}\xi}{2\sqrt{2}\lambda_1}\right)}{\lambda_2}\right). \tag{22}$$

- **Case-3** For $\lambda_2 = 0,\ \lambda_4 = 0,\ \lambda_5 = 0$ and $\lambda_3 > 0$, offers $\alpha_0 = 0,\ \alpha_1 = \frac{a\sqrt{\lambda_1}}{\sqrt{d}},\ b = \frac{1}{2}\left(c^2 - a^2\lambda_3\right)$. we get the exponential function solution:

$$U_9(x,t) = e^{\left(\frac{i\Gamma(\beta+1)\left(cx^{\omega}-\frac{1}{2}t^{\omega}\left(c^2-a^2\lambda_3\right)\right)}{\omega}\right)}\left(\frac{4a\sqrt{\lambda_1}\lambda_3\rho}{\sqrt{d}\left(4\rho^2e^{\sqrt{\lambda_3}\xi}-\lambda_1\lambda_3e^{\sqrt{\lambda_3}(-\xi)}\right)}\right). \tag{23}$$

By taking $\lambda_1 = -\frac{4\rho^2}{\lambda_3}$ in (23), we have the bright-type soliton solution

$$U_{10}(x,t) = e^{\frac{i\Gamma(\beta+1)(cx^{\omega}-bt^{\omega})}{\omega}}\left(\frac{a\lambda_3\sqrt{-\frac{\rho^2}{\lambda_3}}\operatorname{sech}\left(\sqrt{\lambda_3}\xi\right)}{\sqrt{d}\rho}\right). \tag{24}$$

Similarly, by taking $\lambda_1 = \frac{4\rho^2}{\lambda_3}$ in (23), we have

$$U_{11}(x,t) = e^{\frac{i\Gamma(\beta+1)(cx^{\omega}-bt^{\omega})}{\omega}}\left(\frac{a\lambda_3\sqrt{\frac{\rho^2}{\lambda_3}}\operatorname{csch}\left(\sqrt{\lambda_3}\xi\right)}{\sqrt{d}\rho}\right), \tag{25}$$

where ξ is defined in (6).

4.2 Modified Generalized Exponential Rational Function Method

The solution for mGERFM [30] is stated as:

$$\Phi(\xi) = \sum_{j=1}^{n} a_j \left(\frac{\Omega'(\xi)}{\Omega(\xi)}\right)^{j} + \sum_{j=1}^{n} h_j \left(\frac{\Omega'(\xi)}{\Omega(\xi)}\right)^{-j} + a_0, \tag{26}$$

where

$$\Omega(\xi) = \frac{m_1 e^{\aleph_1 \xi} + m_2 e^{\aleph_2 \xi}}{m_3 e^{\aleph_3 \xi} + m_4 e^{\aleph_4 \xi}}. \tag{27}$$

For $n = 1$, (26) is written as:

$$\Phi(\xi) = a_1 \left(\frac{\Omega'(\xi)}{\Omega(\xi)}\right) + h_1 \left(\frac{\Omega'(\xi)}{\Omega(\xi)}\right)^{-1} + a_0. \tag{28}$$

• By putting $m = [1, 1, 1, 0]$ and $\aleph = [0, -1, 0, 0]$, in (27), gives $\Omega(\zeta) = 1 + e^{-\zeta}$, and inserting (28) in (7) offers $a_1 = 2a_0,\ h_1 = 0,\ b = \frac{1}{4}\left(a^2 + 2c^2\right),\ d = \frac{a^2}{4a_0^2}$, then we get:

Soliton solution of exponential form

$$U_1(x,t) = e^{\left(\frac{i\Gamma(\beta+1)\left(cx^{\omega} - \frac{1}{4}\left(a^2+2c^2\right)t^{\omega}\right)}{\omega}\right)} \left(\frac{a_0\left(e^{\frac{a\Gamma(\beta+1)(x^{\omega}-ct^{\omega})}{\omega}} - 1\right)}{e^{\frac{a\Gamma(\beta+1)(x^{\omega}-ct^{\omega})}{\omega}} + 1}\right). \tag{29}$$

The explicit hyperbolic solution

$$U_2(x,t) = e^{\left(\frac{i\Gamma(\beta+1)\left(cx^{\omega} - \frac{1}{4}\left(a^2+2c^2\right)t^{\omega}\right)}{\omega}\right)} \left(a_0 \tanh\left(\frac{a\Gamma(\beta+1)\left(x^{\omega} - ct^{\omega}\right)}{2\omega}\right)\right). \tag{30}$$

• Next, letting $m = [2, 0, 1, 1]$ and $\aleph = [-2, 0, 1, -1]$, in (27), offers $\Omega(\xi) = e^{-2\xi}\,\mathrm{sech}(\xi)$ while solving (28) and $a_1 = 0,\ a_0 = \frac{2h_1}{3},\ b = a^2 + \frac{c^2}{2},\ d = \frac{9a^2}{h_1^2}$, the following solutions are written as:

The dark soliton solution

$$U_3(x,t) = \frac{h_1 \exp\left(\frac{i\Gamma(\beta+1)\left(cx^{\omega} - \frac{1}{2}\left(2a^2+c^2\right)t^{\omega}\right)}{\omega}\right)\left(2\tanh\left(\frac{a\Gamma(\beta+1)(x^{\omega}-ct^{\omega})}{\omega}\right) + 1\right)}{3\left(\tanh\left(\frac{a\Gamma(\beta+1)(x^{\omega}-ct^{\omega})}{\omega}\right) + 2\right)}. \tag{31}$$

• Taking $m = [-i, -i, -i, -i]$ and $\aleph = [1, -1, 0, 0]$, (27), offers $\Omega(\xi) = cosh(\xi)$, (28) and (7) provide $a_1 = \frac{a}{\sqrt{d}},\ a_0 = 0,\ h_1 = \frac{a}{\sqrt{d}},\ b = \frac{1}{2}\left(8a^2 + c^2\right)$, and $a_1 = 0,\ a_0 = 0,\ h_1 = \frac{a}{\sqrt{d}},\ b = a^2 + \frac{c^2}{2}$, implies the following solutions:

$$U_4(x,t) = e^{\left(\frac{i\Gamma(\beta+1)\left(cx^{\omega} - \frac{1}{2}\left(8a^2+c^2\right)t^{\omega}\right)}{\omega}\right)} \left(\frac{a\left(\coth^2\left(\frac{a\Gamma(\beta+1)(x^{\omega}-ct^{\omega})}{\omega}\right) + 1\right)\tanh\left(\frac{a\Gamma(\beta+1)(x^{\omega}-ct^{\omega})}{\omega}\right)}{\sqrt{d}}\right), \tag{32}$$

$$U_5(x,t)=e^{\left(\frac{i\Gamma(\beta+1)\left(cx^{\omega}-\frac{1}{2}\left(8a^2+c^2\right)t^{\omega}\right)}{\omega}\right)}\left(\frac{a\coth\left(\frac{a\Gamma(\beta+1)(x^{\omega}-ct^{\omega})}{\omega}\right)}{\sqrt{d}}\right). \tag{33}$$

• By taking $m=[1,1,1,0]$ and $\aleph=[3,2,0,0]$, (27), offers $\Omega(\zeta)=e^{2\zeta}+e^{3\zeta}$, while (28) and (7) gives $a_1=0,\ a_0=-\frac{1}{12}(5h_1),\ b=\frac{1}{4}\left(a^2+2c^2\right),\ d=\frac{36a^2}{h_1^2}$, and $a_1=0,\ a_0=-\frac{1}{12}(5h_1),\ b=\frac{1}{4}\left(a^2+2c^2\right),\ d=\frac{36a^2}{h_1^2}$, then we get:

$$U_6(x,t)=-e^{\left(\frac{i\Gamma(\beta+1)\left(cx^{\omega}-\frac{1}{4}\left(a^2+2c^2\right)t^{\omega}\right)}{\omega}\right)}\left(\frac{h_1\left(3e^{\frac{a\Gamma(\beta+1)(x^{\omega}-ct^{\omega})}{\omega}}-2\right)}{36e^{\frac{a\Gamma(\beta+1)(x^{\omega}-ct^{\omega})}{\omega}}+24}\right). \tag{34}$$

Next, the hyperbolic solution

$$U_7(x,t)=-e^{\left(\frac{i\Gamma(\beta+1)\left(cx^{\omega}-\frac{1}{4}\left(a^2+2c^2\right)t^{\omega}\right)}{\omega}\right)}\left(\frac{h_1\left(\cosh\left(\frac{\Gamma(\beta+1)(ax^{\omega}-act^{\omega})}{2\omega}\right)+5\sinh\left(\frac{\Gamma(\beta+1)(ax^{\omega}-act^{\omega})}{2\omega}\right)\right)}{12\left(5\cosh\left(\frac{\Gamma(\beta+1)(ax^{\omega}-act^{\omega})}{2\omega}\right)+\sinh\left(\frac{\Gamma(\beta+1)(ax^{\omega}-act^{\omega})}{2\omega}\right)\right)}\right). \tag{35}$$

• Choosing $m=[1,1,2,0]$ and $\aleph=[i,-i,0,0]$, then (27), gives $\Omega(\zeta)=\cos\zeta$, (28) and (7) provide $a_1=\frac{a}{\sqrt{d}},\ a_0=0,\ h_1=-\frac{a}{\sqrt{d}},\ b=\frac{1}{2}\left(c^2-8a^2\right),\ a_1=\frac{a}{\sqrt{d}},\ a_0=0,\ h_1=0,\ b=\frac{1}{2}\left(c^2-2a^2\right)$, and $a_1=0,\ a_0=0,\ h_1=-\frac{a}{\sqrt{d}},\ b=\frac{1}{2}\left(c^2-2a^2\right)$, we get:

$$U_8(x,t)=e^{\left(\frac{i\Gamma(\beta+1)\left(cx^{\omega}-\frac{1}{2}\left(c^2-8a^2\right)t^{\omega}\right)}{\omega}\right)}\left(\frac{a\left(\cot^2\left(\frac{a\Gamma(\beta+1)(x^{\omega}-ct^{\omega})}{\omega}\right)-1\right)\tan\left(\frac{a\Gamma(\beta+1)(x^{\omega}-ct^{\omega})}{\omega}\right)}{\sqrt{d}}\right), \tag{36}$$

$$U_9(x,t)=-e^{\left(\frac{i\Gamma(\beta+1)\left(cx^{\omega}-\frac{1}{2}\left(c^2-8a^2\right)t^{\omega}\right)}{\omega}\right)}\left(-\frac{a\tan\left(\frac{a\Gamma(\beta+1)(x^{\omega}-ct^{\omega})}{\omega}\right)}{\sqrt{d}}\right), \tag{37}$$

$$U_{10}(x,t)=e^{\left(\frac{i\Gamma(\beta+1)\left(cx^{\omega}-\frac{1}{2}\left(c^2-8a^2\right)t^{\omega}\right)}{\omega}\right)}\left(\frac{a\cot\left(\frac{a\Gamma(\beta+1)(x^{\omega}-ct^{\omega})}{\omega}\right)}{\sqrt{d}}\right). \tag{38}$$

4.3 Multivariate Generalized Exponential Rational Integral Function Approach

The general solution to MGERIFM [31] is described as:

$$\Phi(\xi)=c_0+\sum_{r=1}^{n}g_i\left(\underbrace{\iint\cdots\int}_{r}v(\xi)d\xi d\xi\cdots d\xi\right)^{r}+\sum_{r=1}^{n}h_r\left(\underbrace{\iint\cdots\int}_{r}v(\xi)d\xi d\xi\cdots d\xi\right)^{-r}. \tag{39}$$

The solution to equation (39) for $n = 1$ is as follows:

$$\Phi(\xi) = c_0 + g_1 \int v(\xi)d\xi + h_1 \left(\int v(\xi)d\xi\right)^{-1}, \tag{40}$$

where $v(\xi)$ is defined by

$$v(\xi) = \frac{\tau_1 e^{\xi s_1} + \tau_2 e^{\xi s_2}}{\tau_3 e^{\xi s_3} + \tau_4 e^{\xi s_4}}. \tag{41}$$

Moreover, the general solutions can be expressed as:

Case-1: Choosing $[\tau_1, \tau_2, \tau_3, \tau_4] = [-i, -i, -i, -i]$ and $[s_1, s_2, s_3, s_4] = [1, -1, 0, 0]$, (41) takes the following form

$$v(\xi) = \cosh(\xi). \tag{42}$$

Inserting (42) into (40), implies that

$$\Phi(\xi) = c_0 + g_1 \sinh(\xi) + h_1 \sinh^{-1}(\xi). \tag{43}$$

The solutions are as follows when (43) is inserted into (7):

For $c_0 = 0,\ g_1 = 0,\ a = \sqrt{d}h_1,\ b = \frac{1}{2}\left(c^2 - dh_1^2\right)$, we have:

$$U_1(x,t) = e^{\left(\frac{i\Gamma(\beta+1)\left(cx^\omega - \frac{1}{2}t^\omega\left(c^2 - dh_1^2\right)\right)}{\omega}\right)}\left(h_1 \operatorname{csch}\left(\frac{\sqrt{d}h_1\Gamma(\beta+1)\left(x^\omega - ct^\omega\right)}{\omega}\right)\right). \tag{44}$$

Case-2: Let $[\tau_1, \tau_2, \tau_3, \tau_4] = [2i, -2i, 4i, 4i]$ and $[s_1, s_2, s_3, s_4] = \left[\frac{1}{2}, -\frac{1}{2}, 0, 0\right]$, (41) transforms to sine hyperbolic function

$$v(\xi) = \frac{1}{2}\sinh\left(\frac{\xi}{2}\right). \tag{45}$$

Plugging (45) into (40), offers

$$\Phi(\xi) = c_0 + g_1 \cosh\left(\frac{\xi}{2}\right) + h_1 \cosh^{-1}\left(\frac{\xi}{2}\right). \tag{46}$$

Applying (46) to (7), we get:

For $c_0 = 0,\ g_1 = 0,\ d = -\frac{a^2}{4h_1^2},\ b = \frac{1}{8}\left(4c^2 - a^2\right)$, we get the solution as follows:

$$U_2(x,t) = e^{\left(\frac{i\Gamma(\beta+1)\left(a^2 t^\omega - 4c^2 t^\omega + 8cx^\omega\right)}{8\omega}\right)}\left(h_1 \operatorname{sech}\left(\frac{a\Gamma(\beta+1)\left(x^\omega - ct^\omega\right)}{2\omega}\right)\right). \tag{47}$$

Case-3: Taking $[\tau_1, \tau_2, \tau_3, \tau_4] = [1, -1, i, i]$ and $[s_1, s_2, s_3, s_4] = [i, -i, 0, 0]$, (41) converts to the periodic function

$$v(\xi) = \sin(\xi). \tag{48}$$

Putting (48) into (40), gives

$$\Phi(\xi) = c_0 - g_1 \cos(\xi) - h_1 \cos^{-1}(\xi). \tag{49}$$

Incorporating (49) in (7), we have:

For $c_0 = 0,\ g_1 = 0,\ d = \frac{a^2}{h_1^2},\ b = \frac{1}{2}\left(a^2 + c^2\right)$, we obtain:

$$U_3(x,t) = -e^{\left(\frac{i\Gamma(\beta+1)\left(cx^\omega - \frac{1}{2}\left(a^2+c^2\right)t^\omega\right)}{\omega}\right)}\left(h_1 \sec\left(\frac{\Gamma(\beta+1)\left(ax^\omega - act^\omega\right)}{\omega}\right)\right). \tag{50}$$

Case-4: Choosing the parameters $[\tau_1, \tau_2, \tau_3, \tau_4] = [1, 1, 1, 1]$ and $[s_1, s_2, s_3, s_4] = [i, -i, 0, 0]$, (41) offers

$$v(\xi) = \cos(\xi). \tag{51}$$

Manipulating (51) and (40), we have

$$\Phi(\xi) = c_0 + g_1 \sin(\xi) + h_1 \sin^{-1}(\xi). \tag{52}$$

Plugging (52) into (7), give the following solutions:

When $c_0 = 0,\ g_1 = 0,\ b = \frac{1}{2}\left(a^2 + c^2\right),\ d = \frac{a^2}{h_1^2}$, we get:

$$U_4(x,t) = e^{\left(\frac{i\Gamma(\beta+1)\left(cx^\omega - \frac{1}{2}\left(a^2+c^2\right)t^\omega\right)}{\omega}\right)}\left(h_1 \csc\left(\frac{\Gamma(\beta+1)\left(ax^\omega - act^\omega\right)}{\omega}\right)\right). \tag{53}$$

Case-5: Taking the parameters $[\tau_1, \tau_2, \tau_3, \tau_4] = [2, 2, 2, 2]$ and $[s_1, s_2, s_3, s_4] = \left[\frac{2}{5}, \frac{2}{5}, 0, 0\right]$, (41) gives

$$v(\xi) = e^{\frac{2\xi}{5}}. \tag{54}$$

Manipulating (54) and (40), we have

$$\Phi(\xi) = c_0 + \frac{1}{2} g_1 \left(5e^{\frac{2\xi}{5}}\right) + h_1 \left(\frac{5}{2} e^{\frac{2\xi}{5}}\right)^{-1}. \tag{55}$$

Inserting (55) into (7), give the following solution:

When $c_0 = 0,\ d = 0,\ b = \frac{c^2}{2} - \frac{2a^2}{25}$, we get:

$$U_5(x,t) = e^{\left(\frac{i\Gamma(\beta+1)\left(cx^\omega - \left(\frac{c^2}{2} - \frac{2a^2}{25}\right)t^\omega\right)}{\omega}\right)}\left(\frac{5}{2} g_1 e^{\frac{2\Gamma(\beta+1)\left(ax^\omega - act^\omega\right)}{5\omega}} + \frac{2}{5} h_1 e^{-\frac{2\Gamma(\beta+1)\left(ax^\omega - act^\omega\right)}{5\omega}}\right). \tag{56}$$

Next, the hyperbolic solution is written as

$$\begin{aligned} U_6(x,t) = e^{\left(\frac{i\Gamma(\beta+1)\left(cx^\omega - \left(\frac{c^2}{2} - \frac{2a^2}{25}\right)t^\omega\right)}{\omega}\right)} & \left(25 g_1 \left(\cosh\left(\frac{2a\Gamma(\beta+1)\left(x^\omega - ct^\omega\right)}{5\omega}\right)\right.\right. \\ & \left. + \sinh\left(\frac{2a\Gamma(\beta+1)\left(x^\omega - ct^\omega\right)}{5\omega}\right)\right) \\ & \left. + 4h_1 \left(\cosh\left(\frac{2a\Gamma(\beta+1)\left(x^\omega - ct^\omega\right)}{5\omega}\right) - \sinh\left(\frac{2a\Gamma(\beta+1)\left(x^\omega - ct^\omega\right)}{5\omega}\right)\right)\right). \end{aligned} \tag{57}$$

- **Graphical representation**

Characteristics and behaviors of the waves can be observed by representing the solutions in various graph formats. Surface plots can depict the spatial distribution and evolution of the waves, while contour plots can highlight areas with specific wave amplitudes or intensities. Three dimensional plots with color coding can effectively illustrate the interaction between spatial and temporal dimensions, providing a comprehensive depiction of wave dynamics. To show how the new extracted soliton solutions relate to the existing governing equation, we have chosen particular values for the physical parameters in this section. Three-dimensional, graphs two-dimensional and contour plots are used to illustrate how parameters ω and t affect the soliton solutions that are currently in operation. Figures 1, 2, 3, 4 and 5 display 2D, 3D, and contour graphs that illustrate the behavior of the current solutions. Figure 1 represents the behavior of the dark soliton solution for the parameters $\beta = 0.95.c = 1.07, \lambda_1 = 0.9, a = 1.5, \alpha_0 = 2.1, \lambda_2 = 1.9, \lambda_3 = 0.1$. Analyzing and comprehending the dark optical solution is crucial for applications in nonlinear optics, optical communications, and other

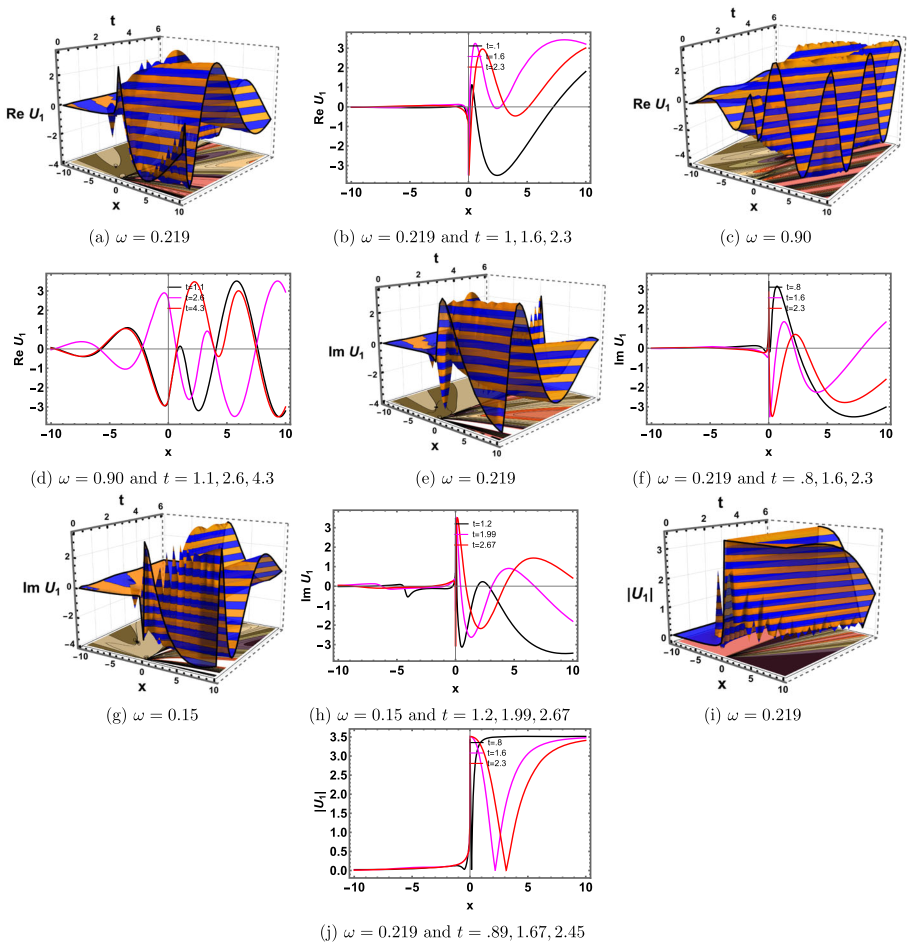

(a) $\omega = 0.219$ (b) $\omega = 0.219$ and $t = 1, 1.6, 2.3$ (c) $\omega = 0.90$

(d) $\omega = 0.90$ and $t = 1.1, 2.6, 4.3$ (e) $\omega = 0.219$ (f) $\omega = 0.219$ and $t = .8, 1.6, 2.3$

(g) $\omega = 0.15$ (h) $\omega = 0.15$ and $t = 1.2, 1.99, 2.67$ (i) $\omega = 0.219$

(j) $\omega = 0.219$ and $t = .89, 1.67, 2.45$

Fig. 1 Plots for the (15) with different parametric values and effect of fractional parameter and time to the dynamics of waves fields requiring exact control and manipulation of light intensity. Figure 2 illustrate the explicit periodic solitary wave for the parameters $\beta = 0.999, c = 2.07, \lambda_1 = 1.9, a = 0.5, \alpha_0 = 0.1, \lambda_2 = 0.9, \lambda_3 = 3.1$. An explicit periodic solitary wave solution can represent a solitary wave that is tuned to periodically recur over an extensive area while maintaining specific properties of a solitary wave, such as a localized concentration of energy. Periodic solitons, also known as cnoidal waves, are solutions that show a periodic confguration in space or time and they grow indefnitely but keep a periodic pattern. Figure 3 shows the bright soliton solution with the assistance of the suitable parameters $a = 1.92, \beta = 0.99, b = 1.2, c = 0.09, d = 0.998, \lambda_3 = 0.02, \rho = 0.2$. Localized waves with a peak that propagate in a nonlinear medium are called bright solitons. They are shown by a localized rise in the field variable, which is the atomic displacement. They merge in environments characterized by focal nonlinearity or dynamic interatomic interactions. In the model under consideration, they are equivalent to localized vibrational modes with an amplitude maximum and subsequent decline from a single location. Moreover, Fig. 4 with the values $a = 1.992, a_0 = 0.098, \beta = 1.09, c = 0.09$ depicts the combined dark bright soltion behavior. Dark solitons, which are localized waves with lower intensity, and bright solitons, which are localized waves with higher intensity, coexist within a single wave function in mixed dark-bright soliton solutions. There are areas in the wave with lower and higher amplitudes or intensities, thus the dark and brilliant parts interact in complicated ways. Figure 5 explains the dynamics of solitary wave for the variables $a = 1, \beta = 0.41, c = 0.69, h_1 = 4.02$. So, soliton behavior can be better understood, analyzed, and optimized with the help of visual representations. It allows for the simplification of difficult ideas, the detection of possible issues (such dispersion or interference), and the creation of efficient and reliable optical communication systems.

5 Qualitative Analysis

In this section, we will discuss the qualitative analysis of the Gross-Pitaevskii equation that includes different tools such as bifurcation, chaotic, sensitivity analysis, using the 2D phase portraits, and time series analysis.

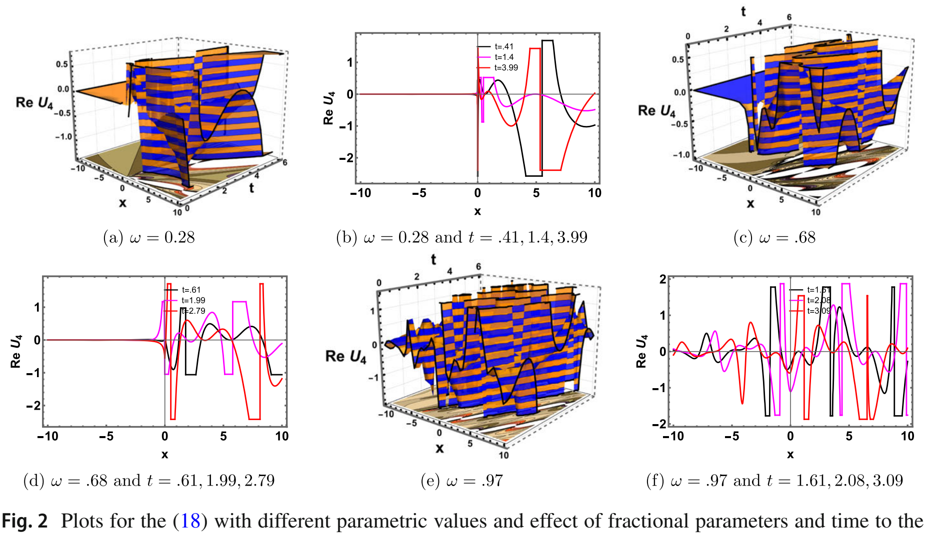

(a) $\omega = 0.28$ (b) $\omega = 0.28$ and $t = .41, 1.4, 3.99$ (c) $\omega = .68$

(d) $\omega = .68$ and $t = .61, 1.99, 2.79$ (e) $\omega = .97$ (f) $\omega = .97$ and $t = 1.61, 2.08, 3.09$

Fig. 2 Plots for the (18) with different parametric values and effect of fractional parameters and time to the dynamics of waves

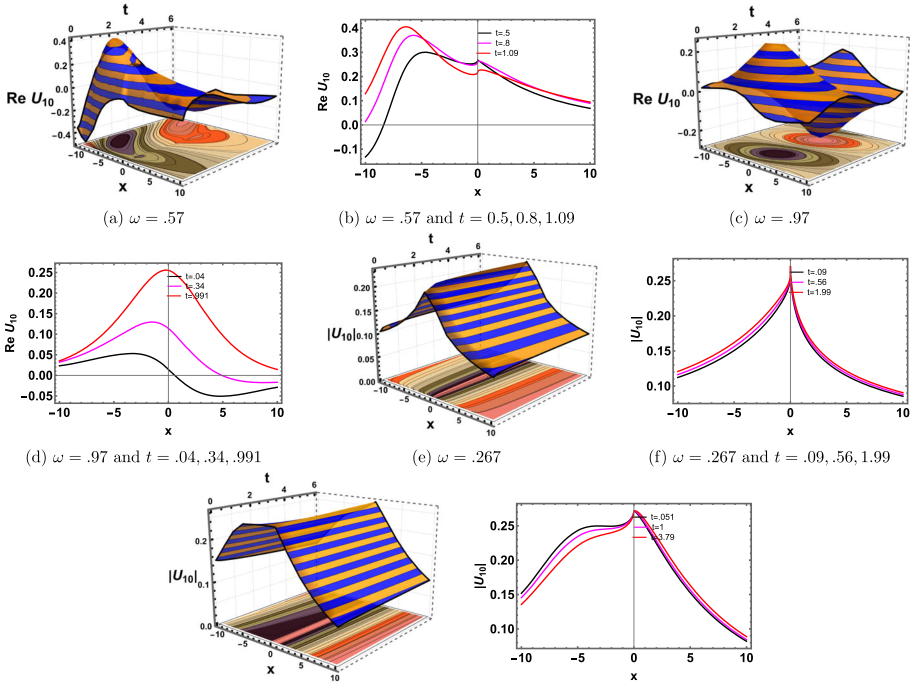

(a) $\omega = .57$ (b) $\omega = .57$ and $t = 0.5, 0.8, 1.09$ (c) $\omega = .97$

(d) $\omega = .97$ and $t = .04, .34, .991$ (e) $\omega = .267$ (f) $\omega = .267$ and $t = .09, .56, 1.99$

(g) $\omega = .66$ (h) $\omega = .66$ and $t = .051, 1, 3.79$

Fig. 3 Plots for the (24) with different parametric values and effect of fractional parameters and time to the dynamics of waves

5.1 Bifurcation Analysis

Bifurcation analysis is a mathematical technique used to study changes in a system's qualitative or topological structure as a parameter within the system is varied. It is commonly applied to nonlinear dynamical systems to understand how their behavior changes as key parameters cross critical thresholds. We discuss the bifurcation analysis of the model using the Galilean transformation on (7), leading to the unperturbed traveling wave system [37, 38, 44–47].

$$\begin{cases} \dfrac{d\Phi}{d\xi} = \mathcal{M}, \\ \dfrac{d\mathcal{M}}{d\xi} = Q_1\Phi(\xi) - Q_2\Phi(\xi)^3. \end{cases} \tag{58}$$

where $Q_1 = \frac{2b-c^2}{a^2}$, $Q_2 = \frac{2d}{a^2}$. The Hamiltonian function of the associated system (58), can be written as:

$$H^{\star}(\Phi, \mathcal{M}) = \frac{\mathcal{M}^2}{2} - Q_1\frac{\Phi^2(\xi)}{2} + Q_2\frac{\Phi^4(\xi)}{4} \ . \tag{59}$$

Where Q_1, Q_2 are the parameters of he dynamical system is described by (58). By solving the system (58) and obtain the following three equilibrium points for system (58) are as follows:

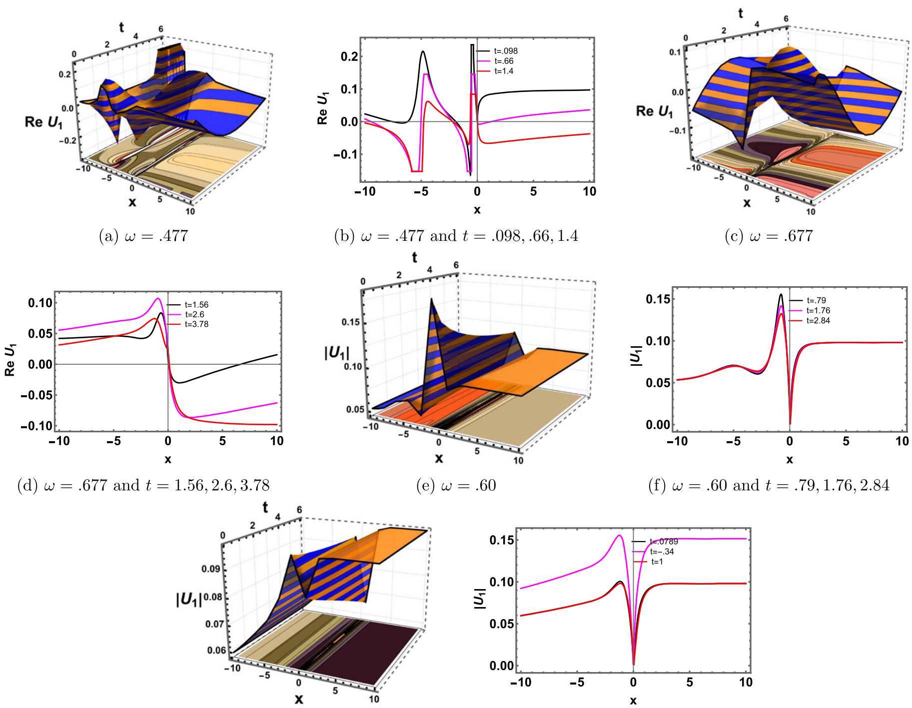

(a) $\omega = .477$ (b) $\omega = .477$ and $t = .098, .66, 1.4$ (c) $\omega = .677$

(d) $\omega = .677$ and $t = 1.56, 2.6, 3.78$ (e) $\omega = .60$ (f) $\omega = .60$ and $t = .79, 1.76, 2.84$

(g) $\omega = .75$ (h) $\omega = .75$ and $t = .0789, .34, 1$

Fig. 4 Plots for the (29) with different parametric values and effect of fractional parameters and time to the dynamics of waves

$$A = (0, 0), \quad B = \left(0, \sqrt{\frac{Q_1}{Q_2}}\right), C = \left(0, -\sqrt{\frac{Q_1}{Q_2}}\right). \tag{60}$$

Jacobian matrix of (59) is given by:

$$J^{\star}(\Phi, \mathcal{M}) = \begin{vmatrix} 0 & 1 \\ Q_1 - 3Q_2\Phi^2(\xi) & 0 \end{vmatrix}$$

$$J^{\star}(\Phi, \mathcal{M}) = -Q_1 + 3Q_2\Phi^2(\xi). \tag{61}$$

Remark:
As we know that.

- If $J(\Phi, \mathcal{M}) < 0$, then $(\Phi, \mathcal{M})$ is a saddle point.
- If $J(\Phi, \mathcal{M}) > 0$, then $(\Phi, \mathcal{M})$ is a centre.
- If $J(\Phi, \mathcal{M}) = 0$, then $(\Phi, \mathcal{M})$ is a cuspidal point.

Family : **1**

When $Q_1 > 0$ and $Q_2 > 0$ then there are three equilibrium points, $A = (0, 0)$, $B = (0, \sqrt{\frac{Q_1}{Q_2}})$, and $C = (0, -\sqrt{\frac{Q_1}{Q_2}})$. For A when $J(A) = -Q_1 < 0$ therefore A is a saddle point. Similiary, for B when $J(B) = 2Q_1 > 0$ therefore B is a centre point and for C when $J(C) = 2Q_1 > 0$ so C is a centre point.

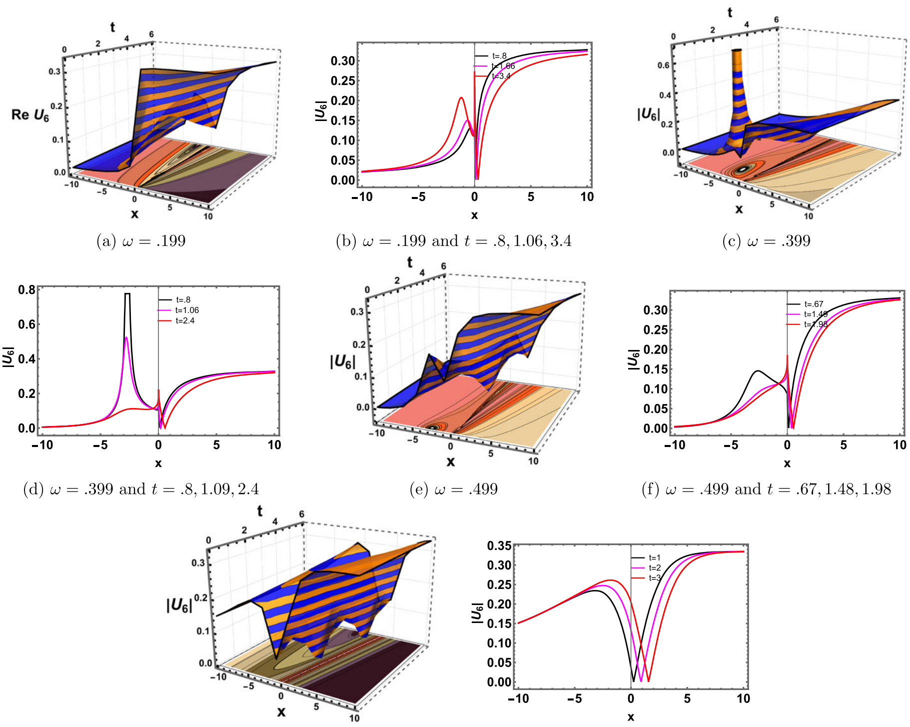

(a) $\omega = .199$ (b) $\omega = .199$ and $t = .8, 1.06, 3.4$ (c) $\omega = .399$

(d) $\omega = .399$ and $t = .8, 1.09, 2.4$ (e) $\omega = .499$ (f) $\omega = .499$ and $t = .67, 1.48, 1.98$

(g) $\omega = .69$ (h) $\omega = .69$ and $t = 1, 2, 3$

Fig. 5 Plots for the (34) with different parametric values and effect of fractional parameters and time to the dynamics of waves

Family : **2**

When $Q_1 > 0$ and $Q_2 < 0$ then there are three equilibrium points, $A = (0, 0)$, $B = (0, \sqrt{\frac{Q_1}{Q_2}})$, and $C = (0, -\sqrt{\frac{Q_1}{Q_2}})$. For A when $J(A) = -Q_1 < 0$ therefore A is a saddle

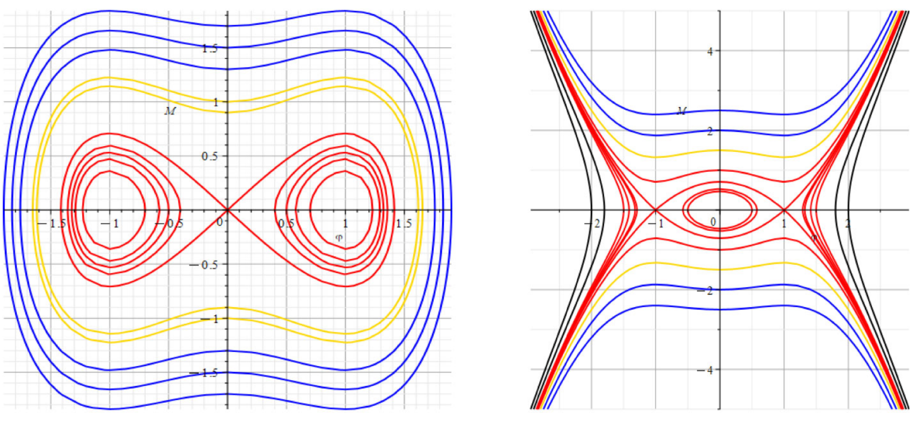

(a) When $Q_1 > 0$ and $Q_2 > 0$ (b) When $Q_1 > 0$ and $Q_2 < 0$

Fig. 6 Diagrams of the bifurcation analysis of the system (58)

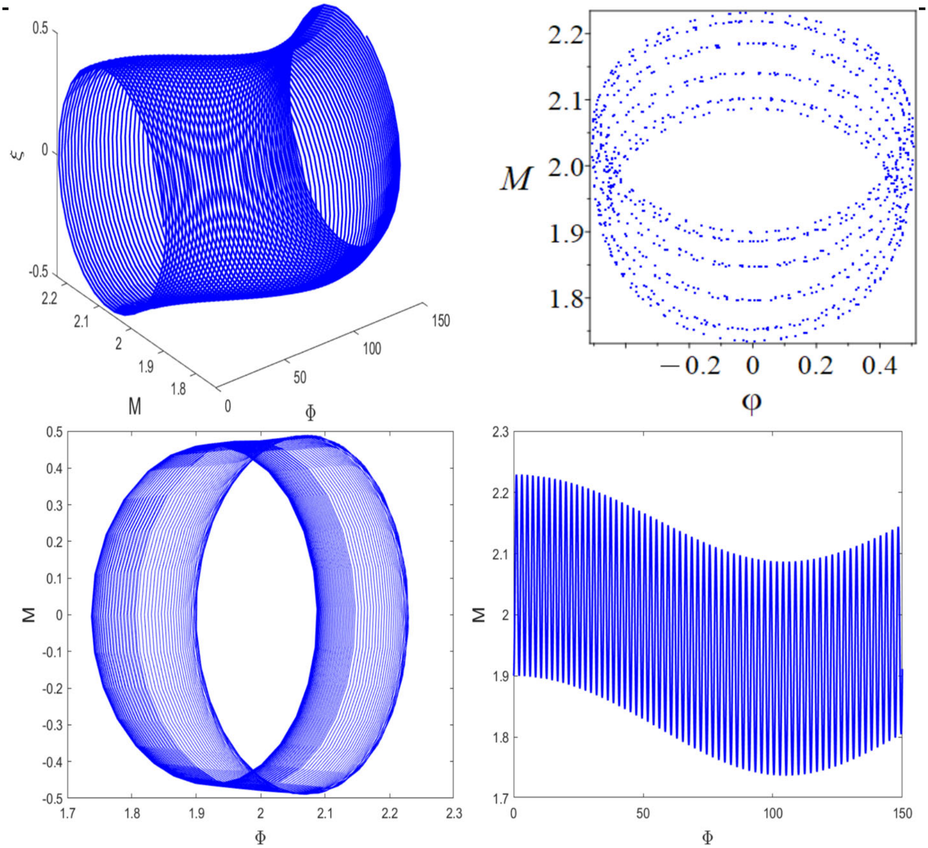

Fig. 7 The chaotic behaviors of (62), when $\mathcal{N}(\xi) = \Omega\cos(\beta\xi)$ by using the suitable parametric values $Q_1 = 4$, $Q_2 = 1$, $\Omega = 0.6$ and $\beta = 0.3$, with initial condition (1.9, 0.01)

point. Similiary, for B when $J(B) = 2Q_1 > 0$ therefore B is a centre point and for C when $J(C) = 2Q_1 > 0$ so C is a centre point.

Family : **3**

When $Q_1 < 0$ and $Q_2 > 0$ then there are three equilibrium points, $A = (0, 0)$, $B = (0, \sqrt{\frac{Q_1}{Q_2}})$, and $C = (0, -\sqrt{\frac{Q_1}{Q_2}})$. For A when $J(A) = Q_1 > 0$ therefore A is a centre point. Similiary, for B when $J(B) = -2Q_1 < 0$ therefore B is a saddle point and for C when $J(C) = -2Q_1 < 0$ so C is a saddle point.

Family : **4**

When $Q_1 < 0$ and $Q_2 < 0$ then there are three equilibrium points, $A = (0, 0)$, $B = (0, \sqrt{\frac{Q_1}{Q_2}})$, and $C = (0, -\sqrt{\frac{Q_1}{Q_2}})$. For A when $J(A) = Q_1 > 0$ therefore A is a centre point. Similiary, For B when $J(B) = -2Q_1 < 0$ therefore B is a saddle point and for C when $J(C) = -2Q_1 < 0$ so C is a saddle point (Fig. 6).

5.2 Qualitative Analysis with Perturbation Term

Chaotic behavior in a dynamical system refers to a type of behavior that appears random and unpredictable, despite being governed by deterministic rules (i.e., no randomness is involved

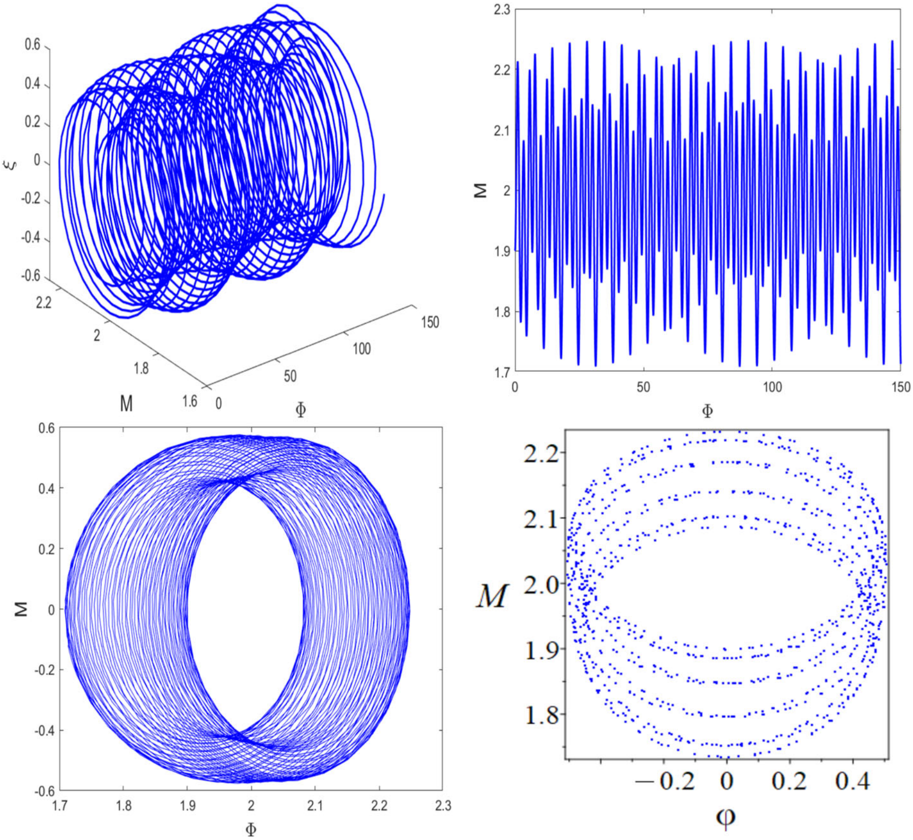

Fig. 8 The chaotic behaviors of (62), when $\mathcal{N}(\xi) = \Omega\cos(\beta\xi)$ by using the suitable parametric values $Q_1 = 4$, $Q_2 = 1$, $\Omega = 0.6$ and $\beta = 0.9$ with same initial condition $(1.9, 0.01)$

in the system's equations). This phenomenon arises in nonlinear systems and is characterized by sensitivity to initial conditions, meaning that even a tiny change in the starting point can lead to drastically different outcomes over time.In this analysis, the dynamical system (58) is influenced by an external force, leading to the modified system (58). Assume that $\Omega\cos(\beta\xi)$ is a perturbation term, and by using the Galilean transformation on (7), then (7) can be converted as follows [39, 40]:

$$\begin{cases} \dfrac{d\Phi}{d\xi} = \mathcal{M}, \\ \dfrac{d\mathcal{M}}{d\xi} = Q_1\Phi(\xi) - Q_2\Phi(\xi)^3 + \mathcal{N}(\xi)\cdot \end{cases} \tag{62}$$

where $Q_1 = \frac{2b-c^2}{a^2}$, $Q_2 = \frac{2d}{a^2}$. Here, the expression $\mathcal{N}(\xi) = \Omega\cos(\beta\xi)$ is referred to as the perturbation where Ω is a amplitude and β is frequency of the system (62) . The investigation keeps all other physical parameters of the system in (62) constant.

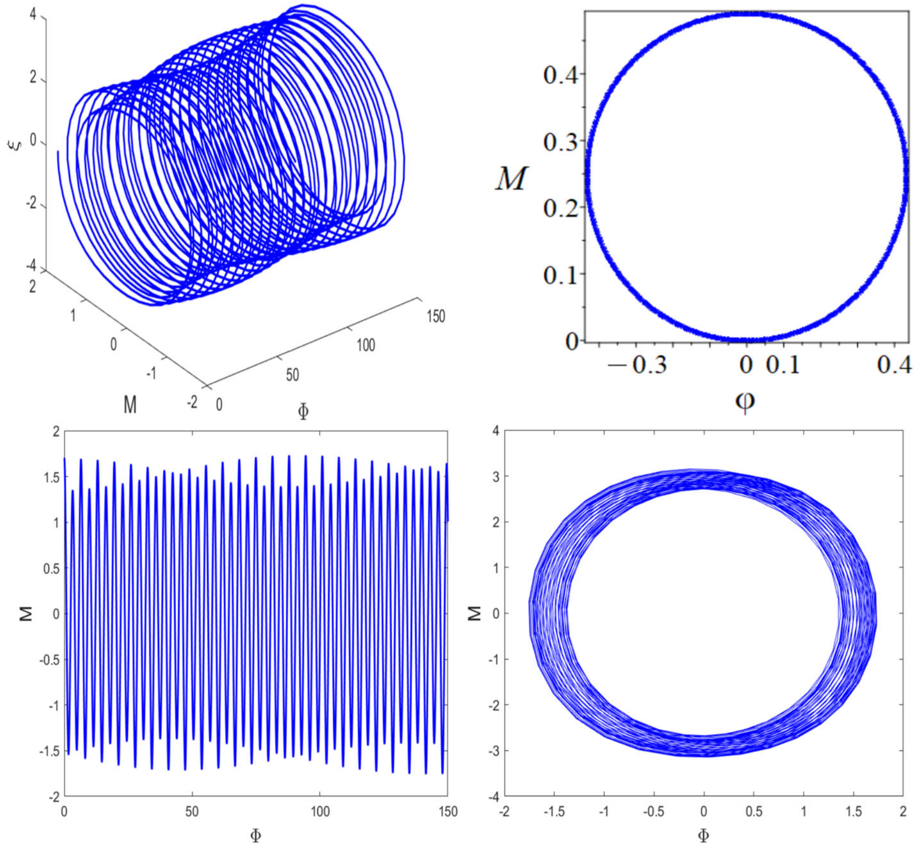

Fig. 9 The chaotic behaviors of (62), when $\mathcal{N}(\xi) = \Omega\cos(\beta\xi)$ by using the suitable parametric values $Q_1 = -3$, $Q_2 = 0.4$, $\Omega = 0.5$ and $\beta = 1$ with initial condition $(1.7, 0.1)$

In our research, we observed chaotic behavior in the system (62), characterized by unpredictable, time-dependent trajectories diverging from regular patterns. We employed a 2D phase portrait, and Poincare mapp time series analysis to detect chaos. We examined the time evolution of these exponents to understand the perturbed dynamical system. By giving the values of the suitable parameters, 2-dimensional, Poincare map and time series analysis of the dynamical system (62) are shown in Figs. 7, 8 and 9.

6 Multi-stability Analysis of the GP Model

The multistability of a system with a perturbed term like (62) will be explored further in this paper. According to [41], multistability refers to multiple solutions for different physical variables and initial conditions in a dynamical system. In Fig. 10, phase portraits (red and green) are plotted for $\Omega = 1.5$ and $\beta = 4.5$, with initial conditions $(\phi, M) = (0.99, 0.01)$ and $(\phi, M) = (0.05, 0.01)$. The system shows quasi-periodic behavior. We also analyze multistability under the same parameters but with different initial conditions, $(\phi, M) = (0.9, 0.01)$ and $(\phi, M) = (0.5, 0.01)$.

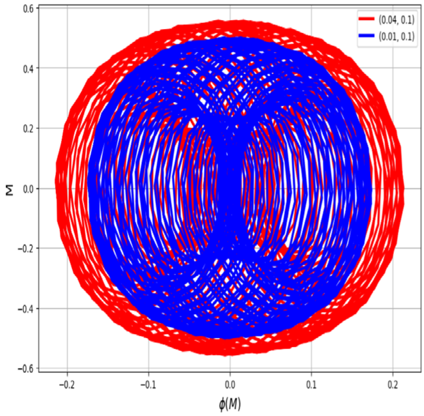

(a) When $(0.99, 0.01)$ and $(0.05, 0.01)$.

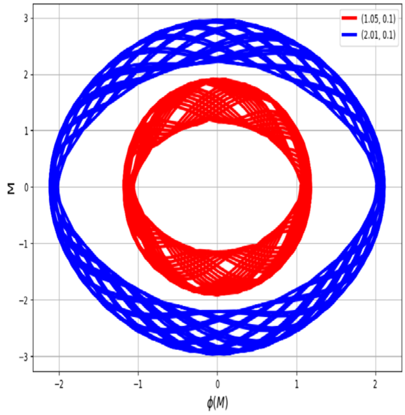

(b) When $(0.9, 0.01)$ and $(0.5, 0.01)$.

Fig. 10 Diagrams of the multistability analysis of the system (62)

7 Sensitivity Visualization of Proposed Model

The sensitivity analysis is under consideration on letting $\Phi' = \mathcal{M}$ by usage of Galilean transformation, so (7) becomes [42, 43]:

$$
\begin{cases}
\dfrac{d\Phi}{d\xi} = \mathcal{M}, \\
\dfrac{d\mathcal{M}}{d\xi} = Q_1\Phi(\xi) - Q_2\Phi(\xi)^3.
\end{cases}
\tag{63}
$$

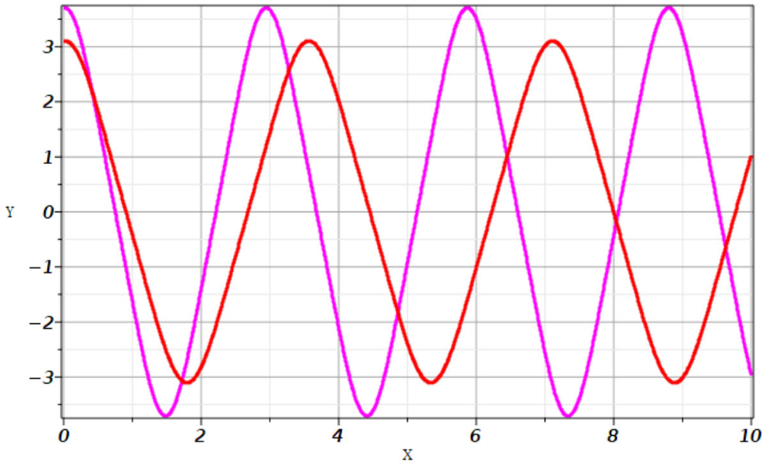

(a) 3D surface plot

Fig. 11 Plots of system (63) with red and magenta with initial condition $(\Phi, \mathcal{M}) = (3.1, 0.3)$ and $(\Phi, \mathcal{M}) = (3.7, 0.5)$ respectively

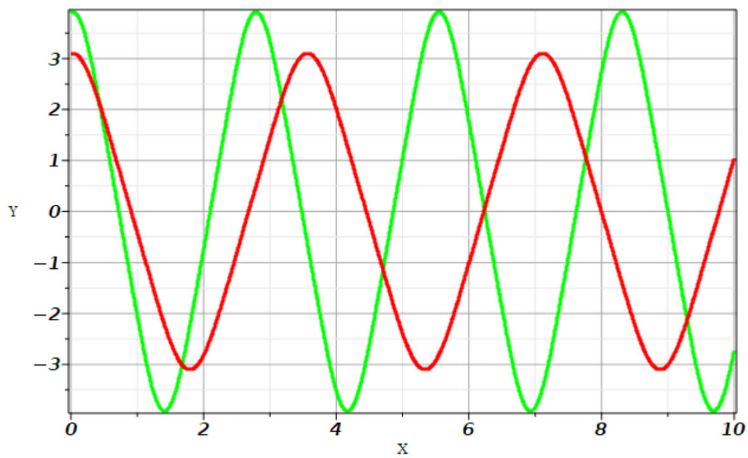

(a) 3D surface plot

Fig. 12 Plots of system (63) with $(\Phi, \mathcal{M}) = (3.9, 0.9)$ in green and $(\Phi, \mathcal{M}) = (3.1, 0.3)$ red (solid) line

where $Q_1 = \frac{2b-c^2}{a^2}$, $Q_2 = \frac{2d}{a^2}$.

Different initial conditions are taken to evaluate system's sensitivity, as depicted in Figs. 11, 12, 13 and 14 while selecting appropriate parameter values $Q_1 = 0.5$ and $Q_2 = 0.3$. In Fig. 11 red and magenta with initial condition $(\Phi, \mathcal{M}) = (3.1, 0.3)$ and $(\Phi, \mathcal{M}) = (3.7, 0.5)$ depicts two different solutions. In Fig. 12 $(\Phi, \mathcal{M}) = (3.9, 0.9)$ in green and $(\Phi, \mathcal{M}) = (3.1, 0.3)$ red (solid) line. In Fig. 13, initial condition $(\Phi, \mathcal{M}) = (3.9, 0.9)$ in green and $(\Phi, \mathcal{M}) = (3.7, 0.5)$ in magenta shows the behavior of two different solutions. Finally, we

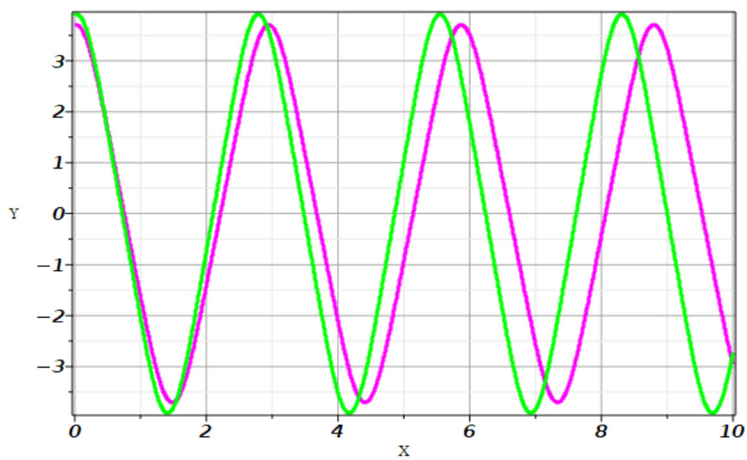

(a) 3D surface plot

Fig. 13 Plots of system (63) with $(\Phi, \mathcal{M}) = (3.9, 0.9)$ in green and $(\Phi, \mathcal{M}) = (3.7, 0.5)$ in magenta show the behavior of two different solutions

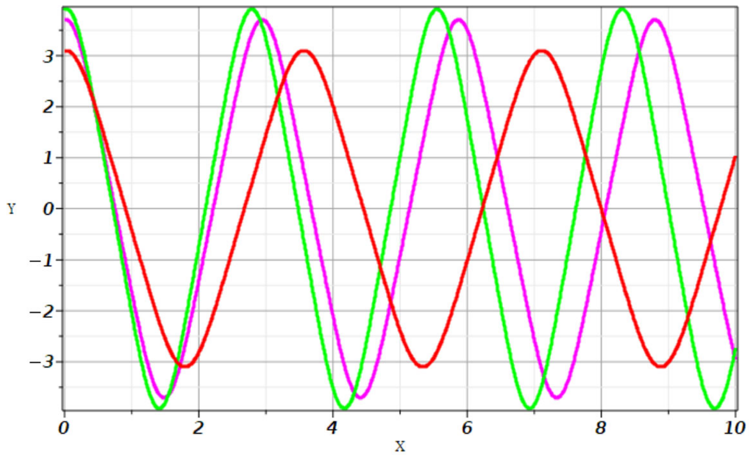

(a) 3D surface plot

Fig. 14 Plots of system (63) with $(\Phi, \mathcal{M}) = (3.9, 0.9)$ in green, $(\Phi, \mathcal{M}) = (3.9, 0.9)$ in magenta and $(\Phi, \mathcal{M}) = (3.1, 0.3)$ red (solid)

check the combination of all the solutions in one Fig. 11 by using the initial conditions $(\Phi, \mathcal{M}) = (3.9, 0.9)$ in green, $(\Phi, \mathcal{M}) = (3.9, 0.9)$ in magenta and $(\Phi, \mathcal{M}) = (3.1, 0.3)$ red (solid).

It has been shown that the solution is not much changed by little variations to the starting values. Consequently, the model under discussion is not very sensitive.

8 Conclusions

Fractional NLPDEs are more broad and flexible than integer-order differential equations. They grow more like classical models as the fractional order approaches unity. In this study, we investigated the nonlinear GPE employing advanced analytical techniques known as Kumar-Malik method, mGERFM and MGERIFM. The GPE is an important model in physics; consequently, its exact soliton solutions are of even greater importance. The results of this paper have theoretically predicted numerous novel nonlinear phenomena in BEC, which are beneficial for our comprehension of certain physical phenomena and experiments in BEC or related disciplines based on the significant nonlinear model in BEC. A variety of solitary wave solutions were extracted and physically depicted in various graphs Figs. 1-5. The fractional and temporal parameter impact have been examined in on optical solutions, providing valuable insights into the importance of the truncated fractional GPE model. Highlighting the role of the M-fractional order parameter represents a significant advancement from previous research, revealing the importance of fractional calculus on the dynamics of solitons. Moreover, in this study, the qualitative analysis together with Galilean transformation was discussed. A variety of aspects like bifurcation analysis, sensitivity analysis, chaotic behavior, 2D, and 3D phase portraits, Poincaré maps, time series analysis, and sensitivity to multistability under the different conditions have been investigated and shown in the Figs. 6-14. Bifurcation analysis is an essential instrument in the examination of dynamical systems and nonlinear events. Understanding stability and key transitions is crucial for anticipating complex system behavior, establishing thresholds and control factors, and gaining insight into nonlinear processes. Poincaré maps serve as an effective instrument in the examination of dynamical systems, especially in the investigation of periodic or quasi-periodic behavior inside continuous-time systems. They offer a method to diminish the dimensional complexity of a system and illustrate its long-term behavior by concentrating on the intersections of trajectories with a lower-dimensional space. Poincaré maps have applications in diverse domains, including physics, engineering, biology, and mathematics. The results are employed to simulate or comprehend certain nonlinear phenomena that manifest during atomic condensation in BEC. This research facilitates the exploration and prediction of potential characteristics and behaviors of relevant models that illustrate physical phenomena, thereby promoting innovation and change in ideas.

Acknowledgements The authors extend their appreciation to King Saud University, for funding this work through Researchers Supporting Project number (RSPD2025R704), King Saud University, Riyadh, Saudi Arabia.

Author Contributions M. Ajmal: Writing-original draft, Methodology; J. Muhammad: Formal analysis, Software; U. Younas: Chaotic Analysis; E. Hussian: Visualization, Validation; M. El-Meligy: Writing - original draft; Writing - review & editing; M. Sharaf: Writing - review, Supervision, Formal analysis

Data Availability No datasets were generated or analysed during the current study.

Declarations

Competing Interests The authors declare no competing interests.

References

1. Leung, A.W.: Systems of nonlinear partial differential equations: Applications to biology and engineering (vol. 49). Springer Science and Business Media (2013)
2. Han, T., Rezazadeh, H., Rahman, M.U.: High-order solitary waves, fission, hybrid waves and interaction solutions in the nonlinear dissipative (2+1)-dimensional Zabolotskaya-Khokhlov model. Phys. Scr. **99**, 115212 (2024)
3. Jin, B., Jin, B.: Cauchy problem for fractional ODEs. Fractional Differential Equations: An Approach via Fractional Derivatives, pp. 97–136 (2021)
4. Wong, P.J.: Applications of Partial Differential Equations. MDPI-Multidisciplinary Digital Publishing Institute (2023)
5. Debnath, L., Debnath, L.: Nonlinear Partial Differential Equations for Scientists and Engineers, pp. 528–529. Birkhäuser, Boston (2005)
6. Mirzazadeh, M., Arnous, A.H., Mahmood, M.F., Zerrad, E., Biswas, A.: Soliton solutions to resonant nonlinear Schrödinger's equation with time-dependent coefficients by trial solution approach. Nonlinear Dyn. **81**, 277–282 (2015)
7. Cattani, C., Sulaiman, T.A., Baskonus, H.M., Bulut, H.: Solitons in an inhomogeneous Murnaghan's rod. Eur. Phys. J. Plus **133**, 1–11 (2018)
8. Arnold, J.M.: Solitons in communications. Electron. Commun. Eng. J. **8**(2), 88–96 (1996)
9. Younas, U., Ren, J., Sulaiman, T.A., Bilal, M., Yusuf, A.: On the lump solutions, breather waves, two-wave solutions of (2+ 1)-dimensional Pavlov equation and stability analysis. Mod. Phys. Lett. B **36**(14), 2250084 (2022)
10. Wan, P., Manafian, J., Ismael, H.F., Mohammed, S.A.: Investigating one-, two-, and triple-wave solutions via multiple exp-function method arising in engineering sciences. Adv. Math. Phys. **2020**(1), 8018064 (2020)
11. Raza, N., Salman, F., Butt, A.R., Gandarias, M.L.: Lie symmetry analysis, soliton solutions and qualitative analysis concerning to the generalized q-deformed Sinh-Gordon equation. Commun. Nonlinear Sci. Numer. Simul. **116**, 106824 (2023)

12. Nasreen, N., Yadav, A., Malik, S., Hussain, E., Alsubaie, A.S., Alsharif, F.: Phase trajectories, chaotic behavior, and solitary wave solutions for (3+ 1)-dimensional integrable Kadomtsev-Petviashvili equation in fluid dynamics. Chaos, Solitons Fractals **188**, 115588 (2024)
13. Zhu, S.D.: The generalizing Riccati equation mapping method in non-linear evolution equation: application to (2+ 1)-dimensional Boiti–Leon–Pempinelle equation. Chaos, Solitons Fractals **37**(5), 1335–1342 (2008)
14. Duan, J.S., Rach, R., Baleanu, D., Wazwaz, A.M.: A review of the Adomian decomposition method and its applications to fractional differential equations. Commun. Fractional Calc. **3**(2), 73–99 (2012)
15. Almusawa, H., Beenish, Jhangeer, A.: Soliton solutions, Lie symmetry analysis and conservation laws of ionic waves traveling through microtubules in live cells. Results Phys. **43**, 106028 (2022)
16. Manas, M.: Darboux transformations for the nonlinear Schrödinger equations. J. Phys. A Math. Gen. **29**(23), 7721 (1996)
17. Hosseini, K., Samadani, F., Kumar, D., Faridi, M.: New optical solitons of cubic-quartic nonlinear Schrödinger equation. Optik **157**, 1101–1105 (2018)
18. Han, T., Jiang, Y., Lyu, J.: Chaotic behavior and optical soliton for the concatenated model arising in optical communication. Results Phys. **58**, 107467 (2024)
19. Han, T., Zhang, K., Jiang, Y., Rezazadeh, H.: Chaotic pattern and solitary solutions for the (21)-dimensional beta-fractional double-chain DNA system. Fractal Fract. **8**(7), 415 (2024)
20. Gu, Y., Chen, B., Ye, F., Aminakbari, N.: Soliton solutions of nonlinear Schrödinger equation with the variable coefficients under the influence of Woods-Saxon potential. Results Phys. **42**, 105979 (2022)
21. Muhammad, J., Ali, Q., Younas, U.: On the analysis of optical pulses to the fractional extended nonlinear system with mechanism of third-order dispersion arising in fiber optics. Opt. Quant. Electron. **56**(7), 1168 (2024)
22. Zayed, E.M.E., Ibrahim, S.H.: Exact solutions of nonlinear evolution equations in mathematical physics using the modified simple equation method. Chin. Phys. Lett. **29**(6), 060201 (2012)
23. Shah, N.A., Agarwal, P., Chung, J.D., El-Zahar, E.R., Hamed, Y.S.: Analysis of optical solitons for nonlinear Schrödinger equation with detuning term by iterative transform method. Symmetry **12**(11), 1850 (2020)
24. Ansari, A.R., Jhangeer, A., Imran, M., Beenish Inc, M.: A study of self-adjointness, Lie analysis, wave structures, and conservation laws of the completely generalized shallow water equation. Eur. Phys. J. Plus **139**(6), 489 (2024)
25. Chen, C., Jiang, Y.L.: Simplest equation method for some time-fractional partial differential equations with conformable derivative. Comput. Math. Appl. **75**(8), 2978–2988 (2018)
26. Jhangeer, A., Beenish.: Ferroelectric frontiers: Navigating phase portraits, chaos, multistability and sensitivity in thin-film dynamics. Chaos, Solitons Fractals **188**, 115540 (2024)
27. Jhangeer, A., Beenish, Říha, L.: Symmetry analysis, dynamical behavior, and conservation laws of the dual-mode nonlinear fluid model. Ain Shams Eng. J. **16**(1), 103178 (2025)
28. Khan, A.Q., Akhtar, T., Jhangeer, A., Riaz, M. B.: Codimension-two bifurcation analysis at an endemic equilibrium state of a discrete epidemic model. AIMS Math. **9**(5), 13006–13027 (2024)
29. Kumar, S., Malik, S.: A new analytic approach and its application to new generalized Korteweg-de Vries and modi ed Korteweg-de Vries equations. Math. Methods Appl. Sci. 1–18 (2024)
30. Rehman, S.U., Ahmad, J., Muhammad, T.: Dynamics of novel exact soliton solutions to stochastic Chiral nonlinear Schrödinger equation. Alex. Eng. J. **79**, 568–580 (2023)
31. Niwas, M., Kumar, S., Rajput, R., Chadha, D.: Exploring localized waves and different dynamics of solitons in (2+ 1)-dimensional Hirota bilinear equation: a multivariate generalized exponential rational integral function approach. Nonlinear Dyn. 1–14 (2024)
32. Sousa, J.V.D.C., de Oliveira, E.C.: A new truncated M-fractional derivative type unifying some fractional derivative types with classical properties. arXiv:1704.08187 (2017)
33. Görlitz, A., Vogels, J.M., Leanhardt, A.E., Raman, C., Gustavson, T.L., Abo-Shaeer, J.R., ... Ketterle, W.: Realization of Bose-Einstein condensates in lower dimensions. Phys. Rev. Lett. **87**(13), 130402 (2001)
34. Gao, W., Baskonus, H.M.: The modulation instability analysis and analytical solutions of the nonlinear Gross-Pitaevskii model with conformable operator and Riemann wave equations via recently developed scheme. Adv. Math. Phys. **2023**(1), 4132763 (2023)
35. Wang, H., Zhou, Q., Liu, W.: Exact analysis and elastic interaction of multi-soliton for a two-dimensional Gross-Pitaevskii equation in the Bose-Einstein condensation. J. Adv. Res. **38**, 179–190 (2022)
36. Yépez-Martínez, H., Alqahtani, R.T.: Analytical soliton solutions for the beta fractional derivative Gross-Pitaevskii system with linear magnetic and time dependent laser interactions. Phys. Scr. **99**(2), 025238 (2024)

37. Hussain, E., Malik, S., Yadav, A., Shah, S.A.A., Iqbal, M.A.B., Ragab, A.E., Mahmoud, H.M.: Qualitative analysis and soliton solutions of nonlinear extended quantum Zakharov-Kuznetsov equation. Nonlinear Dyn. 1–16 (2024)
38. Shah, S.A.A., Hussain, E., Ma, W.X., Li, Z., Ragab, A.E., Khalaf, T.M.: Qualitative analysis and new variety of solitons profiles for the (1+ 1)-dimensional modified equal width equation. Chaos, Solitons Fractals **187**, 115353 (2024)
39. Li, Z., Hussain, E.: Qualitative analysis and optical solitons for the (1+ 1)-dimensional Biswas-Milovic equation with parabolic law and nonlocal nonlinearity. Results Phys. **56**, 107304 (2024)
40. Li, Z., Lyu, J., Hussain, E.: Bifurcation, chaotic behaviors and solitary wave solutions for the fractional Twin-Core couplers with Kerr law non-linearity. Sci. Rep. **14**(1), 22616 (2024)
41. Jhangeer, A., Ansari, R., A., Abdul Rahimzai, A., Beenish, Qadeer Khan, A.: Exploring chaos and sensitivity in the Ivancevic option pricing model through perturbation analysis. PLoS One **19**(11), e0312805 (2024)
42. Hussain, E., Li, Z., Shah, S.A.A., Az-Zo'bi, E.A., Hussien, M.: Dynamics study of stability analysis, sensitivity insights and precise soliton solutions of the nonlinear (STO)-Burger equation. Opt. Quant. Electron. **55**(14), 1274 (2023)
43. Hussain, E., Mutlib, A., Li, Z., E. Ragab, A., Shah, S.A.A., Az-Zo'bi, E.A., Raees, N.: Theoretical examination of solitary waves for Sharma-Tasso-Olver Burger equation by stability and sensitivity analysis. Z. Angew. Math. Phys. **75**(3), 96 (2024)
44. Hosseini, K., Hinçal, E., Alizadeh, F., Baleanu, D., Osman, M.S.: Bifurcation analysis, sensitivity analysis, and Jacobi elliptic function structures to a generalized nonlinear Schrödinger equation. Int. J. Theoretical Phys. **63**, 306 (2024)
45. Alizadeh, F., Hosseini, K., Sirisubtawee, S., Hincal, E.: Classical and nonclassical Lie symmetries, bifurcation analysis, and Jacobi elliptic function solutions to a 3D-modified nonlinear wave equation in liquid involving gas bubbles. Boundary Value Probl. **2024**, 111 (2024)
46. Hosseini, K., Alizadeh, F., Hinçal, E., Kaymakamzade, B., Dehingia, K., Osman, M.S.: A generalized nonlinear Schrödinger equation with logarithmic nonlinearity and its Gaussian solitary wave. Opt. Quant. Electron. **56**, 929 (2024)
47. Han, T., Jiang, Y.: Bifurcation, chaotic pattern and traveling wave solutions for the fractional Bogoyavlenskii equation with multiplicative noise. Phys. Scr. **99**(3), 035207 (2024)